DFT Studies of the σ-Donor/π-Acceptor Properties of $[SnCB_{10}H_{11}]^-$ and its Relationship to $[SnCl_3]^-$, CO, PF_3, $[SnB_{11}H_{11}]^{2-}$, $SnC_2B_9H_{11}$ and Related $SnC_2B_nH_{n+2}$ Compounds*

Mark A. Fox, Todd B. Marder, and Lars Wesemann

Abstract: The 1,2-carbastanna-closo-dodecaborate, $[SnCB_{10}H_{11}]^-$, was found via DFT calculations, to have intermediate σ-donor/π-acceptor properties between those of $[SnB_{11}H_{11}]^{2-}$ and 3,1,2-$SnC_2B_9H_{11}$, and quite similar HOMO and LUMO energies and shapes to those of $[SnCl_3]^-$, a stronger σ-donor and weaker π-acceptor than CO or PF_3. The non-carbon containing cluster $[SnB_{11}H_{11}]^{2-}$ is shown to be a very strong donor, whereas the dicarbon cluster 3,1,2-$SnC_2B_9H_{11}$ is a poor σ-donor but good Lewis acid, consistent with experimental results. Thus, these systems can be tuned across a very wide range via isolobal replacement of $[BH]^-$ for CH vertices. The higher negative charge in the non-carbon containing systems, as well as the fact that boron is more electropositive than carbon, contribute to the increased energies of both HOMO and LUMO in the stannaboranes compared with the stannacarboranes, explaining their relative donor and acceptor properties.

M.A. Fox,[1] T.B. Marder,[1] Department of Chemistry, Durham University, South Road, Durham, DH1 3LE, UK.
L. Wesemann, Institüt für Anorganishe Chemie, Universität Tübingen, Auf der Morgenstelle 18, D-72076 Tübingen, Germany

[1]Corresponding authors: MAF: e-mail: m.a.fox@durham.ac.uk, TBM: e-mail: todd.marder@durham.ac.uk

Introduction

Recently, one of us reported (1) the synthesis and coordination chemistry of the new 1,2-carbastanna-closo-dodecaborate, $[SnCB_{10}H_{11}]^-$, and we were intrigued by the structure of the unusual dianion $[Rh(PPh_3)_2(SnCB_{10}H_{11})_3]^{2-}$ (**1**), which has a trigonal bipyramidal geometry with axial PPh_3 ligands and equatorial anionic $SnCB_{10}H_{11}$ ligands, formed from the reaction of Wilkinson's catalyst $[Rh(PPh_3)_3Cl]$ with three equivalents of the anion $[SnCB_{10}H_{11}]^-$. In a d^8-ML_5 trigonal bipyramidal Rh(I) complex, it is well known that the strongest σ-donors occupy axial positions, whereas the strongest π-acceptors occupy equatorial positions, the latter due to the fact that the HOMO for a C_{2v}- d^8-ML_4 fragment is a π-orbital lying in the equatorial plane (2). Thus, it would appear that the anionic $[SnCB_{10}H_{11}]^-$ ligand must be a reasonably strong π-acceptor. It was noted that the structure resembles that proposed for $[Rh(CNcy)_2(SnCl_3)_3]^-$, for which the authors had pointed out (3) that the $SnCl_3$ must be the stronger π-acceptor and CNcy (cyclohexyl isonitrile) must be the stronger σ-donor. In

addition, we noted the similarity of the value of J_{Rh-P} of 88 Hz for **1** to that of 72 Hz reported (4) for $[Rh(PPh_3)_2(CO)_3]^+$, (**2**), which also has a (fluxional) tbp geometry, with axial PPh_3 groups and equatorial CO ligands, as expected. That the J_{Rh-P} value for **1** was slightly larger than that for **2** suggested that the $[SnCB_{10}H_{11}]^-$ ligand was probably a stronger σ-donor and weaker π-acceptor than CO. Nonetheless, it was clear that the $[SnCB_{10}H_{11}]^-$ ligand must be a reasonably strong π-acceptor for all three of them to occupy equatorial positions. Before we begin a detailed examination of the frontier orbitals of the $[SnCB_{10}H_{11}]^-$ ligand, it is worth pointing out that the isoelectronic dianionic stannaborane $[SnB_{11}H_{11}]^{2-}$ ligand (5,6) is strongly nucleophilic at the tin center, exhibits an extremely strong *trans*-influence, and forms numerous transition metal coordination complexes (7,8), including such unusual homoleptic species as $[M(SnB_{11}H_{11})_4]^{4-}$ and $[M(SnB_{11}H_{11})_6]^{8-}$ (M = Ni, Pd, Pt) (9), the latter complexes involving the Group 10 metals in their formal IV oxidation state. In contrast, the neutral analogue (10,11), 3,1,2-$SnC_2B_9H_{11}$ is distinctly electrophilic. Considering this to be a possible stable stannylene analogue, as early as 1976, one of us attempted to coordinate it to photochemically generated $Cr(CO)_5(THF)$ but we were unsuccessful in obtaining evidence for a Cr-Sn complex (12). Indeed, it is now known (13,14) that 1,2-Me_2-3,1,2-$SnC_2B_9H_9$ is capable of binding either one or two N, O, or P-ligands at the Sn-center to provide slipped-stannacarboranes. Likewise, C-substituted analogues of the smaller $SnC_2B_4H_6$ system also bind ligands such as 2,2'-bipyridine and 2,2'-bipyrimidine (15-18), but do not react with $BH_3·THF$ or BF_3 to form adducts (19). The lack of σ-donating ability of the $SnC_2B_4H_{6-n}R_n$ systems was ascribed to the diffuse nature of the exo-polyhedral lone-pair on the tin center (19) and to the symmetric electron distribution in some of the lower lying filled M.O.s which the authors associated with the Sn 'lone pair' (15). In their MNDO calculations on $SnC_2B_4H_6$ (15), the authors indicated that the HOMO is localized on the cage borons. We show below, via DFT MO calculations, that $[SnCB_{10}H_{11}]^-$ has intermediate σ-donor/π-acceptor properties between those of $[SnB_{11}H_{11}]^{2-}$ and 3,1,2-$SnC_2B_9H_{11}$, and quite similar HOMO and LUMO energies and shapes to those of $[SnCl_3]^-$, a stronger σ-donor and weaker π-acceptor than CO or PF_3. We also report the shapes, energies and atomic compositions of the orbitals for these systems as well as for related dicarbastannaboranes (13-24).

Computational Details

All *ab initio* computations were carried out with the Gaussian 03 package (25). The geometries of the six compounds described here were optimised using the B3LYP functional (26) with no symmetry constraints. The basis sets used here were 6-31G* for all atoms (27) except for Sn, for which the LANL2DZ basis set (28) incorporating pseudopotentials was employed. Frequency calculations were performed using these optimised geometries at the same levels of theory, and the lack of any imaginary frequencies confirms that all optimised geometries are true minima. The MO diagrams and orbital contributions were generated with the aid of the Gabedit (29) and GaussSum (30) packages, respectively. Total energies in hartrees for the compounds are: $[SnB_{11}H_{11}]^{2-}$ -283.57267, [2,1-$SnCB_{10}H_{11}]^-$ -296.87390, 3,1,2-$SnC_2B_9H_{11}$ -310.00074, 1,2-Me_2-3,1,2-$SnC_2B_9H_9$ -388.62055, 1,2,3-$SnC_2B_8H_{10}$ -284.53253, 1,2,3-$SnC_2B_4H_6$ -182.63195(0), 1,2,4-$SnC_2B_4H_6$ -182.65517, 4,1,6-$SnC_2B_{10}H_{12}$ -335.45961, 1,6-Me_2-4,1,6-$SnC_2B_{10}H_{10}$ 414.083627, 1,2-μ-$(CH_2CH=CHCH_2)$-4,1,2-$SnC_2B_{10}H_{12}$ -490.26082, $[SnCl_3]^-$ -1384.20488, PF_3 -640.95647, CO -113.30945. The computed Sn bond distances for 1,2,4-$SnC_2B_4H_6$ are Sn-C(2,4) 2.412, Sn-B(3) 2.467 and Sn-B(5,6) 2.431 Å. Calculated Sn bond distances for 1,2-μ-$(CH_2CH=CHCH_2)$-4,1,2-$SnC_2B_{10}H_{10}$ are Sn-C(1,2) 2.437, Sn-B(3,6) 2.434 and Sn-B(7,10) 2.380 Å, using a cage numbering scheme described elsewhere (31).

Calculated NMR shifts at the GIAO-B3LYP level were obtained from the optimised geometries using the same basis sets. Theoretical [11]B chemical shifts at the GIAO-B3LYP level were referenced to B_2H_6 (16.6 ppm) and converted to the usual $BF_3·OEt_2$ scale: $\delta(^{11}B) = 110.0 - \sigma(^{11}B)$. The ^{13}C and ^{1}H chemical shifts were referenced to TMS: $\delta(^{13}C) = 189.1 - \sigma(^{13}C)$; $\delta(^1H) = 32.15 - \sigma(^1H)$. Agreements between observed and calculated ^{11}B (and ^{13}C) NMR shifts generated from optimised geometries are generally very good for heteroboranes (32). Agreements between observed and calculated ^{1}H NMR shifts in heteroboranes are often not as good due to a narrow ppm range (ca 12 ppm) and substantial solvent effects on ^{1}H shift measurements (33). Calculated ^{1}H NMR shifts for the hydrogens attached to cage carbons are also in very good agreement with observed data as shown in Table 9. However, hydrogens attached to cage borons have been assigned only for one closo-carbastannaborane, 1,2,3-$SnC_2B_8H_{10}$, and in this case the agreement between computed and observed shifts is surprisingly poor. Agreements between observed and calculated ^{119}Sn NMR shifts are poor due to two factors. The ^{119}Sn NMR shift measurements depend strongly on the solvent, and the pseudopotentials used and the basis set for Sn to compute ^{119}Sn NMR shifts are not considered to be appropriate (34).

Results and Discussion

Our main interest in these systems was to compare the frontier orbitals and σ-donor/π-acceptor abilities of a series of isoelectronic stannaboranes and stannacarboranes containing 1 tin and 0, 1, or 2 carbon atoms in the cage and, especially, to examine those of $[SnCB_{10}H_{11}]^-$, which seemed, on the basis of the reported structure of the rhodium complex **1**, *vide supra*, to have both good σ-donor and π-acceptor properties (1). The metal complexes and borane ligands of interest here are shown in Scheme 1. Optimised geometries of $[SnB_{11}H_{11}]^{2-}$ and [2,1-$SnCB_{10}H_{11}]^-$ at the DFT level of theory are in excellent agreement with their X-ray determined (1,6) molecular structures as demonstrated by comparison of bond lengths involving the tin atom listed in Table 1. However, the dicarbastannaborane, 3,1,2-$SnC_2B_9H_{11}$, and its dimethyl derivative have not been structurally

characterized. The optimised geometry of 3,1,2-SnC$_2$B$_9$H$_{11}$ reveals a slipped Sn vertex with Sn-C bonds being longer than Sn-B bonds, and the trend of the Sn vertex slippage is evident on going from [SnB$_{11}$H$_{11}$]$^{2-}$, to [2,1-SnCB$_{10}$H$_{11}$]$^-$ and 3,1,2-SnC$_2$B$_9$H$_{11}$.

Plots of the frontier orbitals of [SnB$_{11}$H$_{11}$]$^{2-}$, [SnCB$_{10}$H$_{11}$]$^-$, and 3,1,2-SnC$_2$B$_9$H$_{11}$ are displayed in Figure 1, and their energies and coefficients (on Sn, CH, upper belt BH, lower belt BH, and unique BH vertices) are given in Tables 2-4, respectively. For comparison, the frontier orbitals of the well-known π-acceptor ligands [SnCl$_3$]$^-$, PF$_3$, and CO are displayed in Figure 2, and their energies are given in Tables 5-7, respectively. These all have non-degenerate, σ-symmetry HOMOs and degenerate, π-symmetry LUMOs, and the similarity of their orbitals is quite obvious. Their σ-donating ability decreases and their π-accepting ability increases in the order [SnCl$_3$]$^-$, PF$_3$, CO, as evidenced by the orbital energies listed in Tables 5-7.

Noting that [SnB$_{11}$H$_{11}$]$^{2-}$ has five-fold symmetry, belonging to the point group C$_{5v}$, and thus, the LUMO is doubly degenerate (shown in Figure 1 and Table 2 as LUMO and LUMO+1 for consistency), whereas for [SnCB$_{10}$H$_{11}$]$^-$ and 3,1,2-SnC$_2$B$_9$H$_{11}$, the only symmetry element is a mirror plane, and thus, in the C$_s$ point group, there are no degeneracies, one can still see right away the general similarities of the orbital shapes. It is important to note also that for [SnB$_{11}$H$_{11}$]$^{2-}$, while the HOMO is largely of π-symmetry and is heavily localized on the upper belt of the cage, lying at nearly the same in energy are two degenerate and effectively σ-symmetry orbitals. Thus, we will consider the HOMO-1 and HOMO-2 orbitals for this ligand as those suitable for σ-donation to a metal center. We can see, from Table 2, that the HOMO-1 and HOMO-2 orbitals are comprised of a mixture of mainly Sn and the top belt of the cage, but lie at very high energy (+1.43 eV), and are thus both strong donor levels, well above that of [SnCl$_3$]$^-$ (-2.45 eV). The degenerate LUMO orbitals are of π-symmetry, but are also quite high in energy, lying at +7.23 eV, well above those of CO (-0.59 eV), and are thus too high to act as π-acceptor levels, although they are almost completely localized on Sn.

An examination of the two carbon-containing cages, [SnCB$_{10}$H$_{11}$]$^-$ and 3,1,2-SnC$_2$B$_9$H$_{11}$, shows that they have very similar frontier orbitals (Figure 1) comprising an essentially σ-symmetry HOMO and the non-degenerate π-symmetry LUMO and LUMO+1 levels. While the σ-symmetry HOMO, in each case, is slightly 'tipped' towards the carbon vertices, nonetheless, these are of suitable symmetry and have at least modest (46% and 39%, respectively) Sn-content to act as potential σ-donors. For comparison, the σ-donor HOMO levels of [SnCl$_3$]$^-$, PF$_3$, and CO are 45% localized on Sn, 64% localized on P, and 90% localized on C, respectively. Thus, while the HOMO of 3,1,2-SnC$_2$B$_9$H$_{11}$ lies at -7.33 eV, which is below that of [SnCl$_3$]$^-$ (-2.45 eV), but above that of PF$_3$ (-8.78 eV), and CO (-10.11 eV), the combination of relatively low energy and diminished content on the potential donor atom make this a poor σ-donor. In contrast, the LUMO and LUMO+1 energies of 3,1,2-SnC$_2$B$_9$H$_{11}$ are well below those of any of the 'conventional' π-acceptor ligands, and are 87 and 76% localized on Sn, which makes them directly susceptible to nucleophilic attack by one or two Lewis basic ligands.

Now it is useful to consider the case of [SnCB$_{10}$H$_{11}$]$^-$ in more detail. Both the HOMO and LUMO/LUMO+1 orbital energies are in between those of [SnB$_{11}$H$_{11}$]$^{2-}$ and 3,1,2-SnC$_2$B$_9$H$_{11}$, and their Sn-contents are 46, 84, and 77%, respectively (cf. [SnCl$_3$]$^-$, for which the Sn-content of the HOMO is 45%, and the degenerate LUMO is 95%). A comparison of the orbital energies of [SnCB$_{10}$H$_{11}$]$^-$ and [SnCl$_3$]$^-$ is also informative, and we see that these are also quite similar, with the HOMO of the former being -2.87 eV and the latter being -2.45 eV, and for the LUMOs, these values are +2.45 and +2.93 for the former, and +3.25 eV for the latter. [SnCB$_{10}$H$_{11}$]$^-$ would be expected to be a slightly poorer σ-donor and slightly better π-acceptor than [SnCl$_3$]$^-$, but the differences are both small! Thus, [SnCB$_{10}$H$_{11}$]$^-$ and [SnCl$_3$]$^-$ are very similar ligands, both with regard to their energies and orbital overlaps with a metal center. Therefore, it is not surprising to find that it is possible to prepare trigonal bipyramidal Rh(I) complexes bearing three [SnCB$_{10}$H$_{11}$]$^-$ ligands, or that they should all lie in the equatorial plane, as expected for strong π-acceptor ligands.

While only one cage geometry of each of the closo systems, the [SnB$_n$H$_n$]$^{2-}$ dianions and the [SnCB$_n$H$_{n+1}$]$^-$ anions, is known, there are many different geometries of SnC$_2$B$_n$H$_{n+2}$ clusters with n = 4, 8, 9 and 10 reported in the literature (13-24). Molecular structures of dicarbastannaboranes with n = 4 and n = 10 have been structurally characterised (13,15,18,22) and optimised geometries for each system are in very good agreement with experimental data (Table 1). The crystallographically determined molecular structures of the supraicosahedral stannacarboranes, 4,1,6-SnC$_2$B$_{10}$H$_{12}$ and 1,6-Me$_2$-4,1,6-SnC$_2$B$_{10}$H$_{10}$, contain asymmetrical geometries in the solid state which are in excellent agreement with optimized 'gas-phase' calculated geometries, as shown in Table 1 for the Sn-C and Sn-B bond lengths in 1,6-Me$_2$-4,1,6-SnC$_2$B$_{10}$H$_{10}$ (22). One cage carbon is a 4-connected vertex and the other carbon is a 5-connected vertex. Agreement between experimental and optimized geometries for 2-Me$_3$Si-1,2,3-SnC$_2$B$_4$H$_5$ is also very good as shown in Table 1 (13,15). The slippage of the Sn vertices for the 2-Me$_3$Si-1,2,3-SnC$_2$B$_4$H$_5$ geometries is rather less pronounced than for the optimized geometries of 3,1,2-SnC$_2$B$_9$H$_{11}$ and 1,2-Me$_2$-3,1,2-SnC$_2$B$_9$H$_9$.

Geometry optimisations of known SnC$_2$B$_n$H$_{n+2}$ systems with n = 4, 8 and 10 were carried out and the electronic structures at these geometries were examined. The orbitals and their energies for these neutral systems are all similar to 3,1,2-

$SnC_2B_9H_{11}$ (Table 8). This is perhaps not surprising as these systems exhibit similar Lewis acid properties. On this basis, the unknown non-icosahedral $[SnB_nH_n]^{2-}$ and $[SnCB_nH_{n+1}]^-$ ligands would be expected to have similar donor and acceptor properties to those of the icosahedral systems $[SnB_{11}H_{11}]^{2-}$ and $[SnCB_{10}H_{11}]^-$, respectively.

If ^{11}B and ^{13}C NMR shifts computed from an optimized geometry of a heteroborane at the DFT or MP2 level of theory show a very good correlation with its experimental solution-state NMR data then the optimized geometry is considered the best representation of its molecular structure in solution (32). Comparison of the observed and computed ^{11}B and ^{13}C NMR data listed in Table 9 reveals that the optimised geometries of the 12-vertex dicarbastannaboranes 3,1,2-$SnC_2B_9H_{11}$ and 1,2-Me_2-3,1,2-$SnC_2B_9H_9$ with slipped tin vertices are also likely to be found in solution.

However, the calculated ^{11}B and ^{13}C NMR data from the asymmetrical 'gas-phase' optimized geometry of the supraicosahedral system 4,1,6-$SnC_2B_{10}H_{12}$ are in poor agreement with the observed solution NMR data (22). This 13-vertex dicarbastannaborane 4,1,6-$SnC_2B_{10}H_{12}$ is fluxional in solution, interconverting between two mirror related isomers of the asymmetric geometry via a double diamond-square process with a C_s symmetry transition state (22). Averaging of the computed NMR shifts of the relevant pairs of atoms gave very good agreement with the experimental values listed in Table 9, consistent with the fluxionality of the supraicosahedral cluster taking place in solution. The 11-vertex dicarbastannaborane 1,2,3-$SnC_2B_8H_{10}$ has the expected closo-11-vertex geometry based on the excellent agreement between the experimentally assigned solution-state (23) and computed ^{11}B NMR data (Table 9). The optimised geometry reveals short Sn-C bond distances of 2.265 and long Sn-B bond distances of 2.695 Å compared to the corresponding bond distances listed in Table 1. Of interest are the calculated ^{13}C NMR chemical shifts for the two 4-connected carbon vertices in 1,2,3-$SnC_2B_8H_{10}$ (105.8 ppm) and the 4-connected carbon vertex in 4,1,6-$SnC_2B_{10}H_{12}$ (118.3 ppm) which are significantly different from those 5-connected vertices in other stannacarboranes (47.7-65.2 ppm) listed in Table 9.

Conclusions

DFT MO calculations show that $[SnCB_{10}H_{11}]^-$ has intermediate σ-donor/π-acceptor properties between those of the very strong σ-donor $[SnB_{11}H_{11}]^{2-}$ and the poor donor but good Lewis acid 3,1,2-$SnC_2B_9H_{11}$, and quite similar HOMO and LUMO energies and shapes to those of $[SnCl_3]^-$, a stronger σ-donor and weaker π-acceptor than CO or PF_3. Other $SnC_2B_nH_{n+2}$ systems show similar HOMO and LUMO energies to those of 3,1,2-$SnC_2B_9H_{11}$, both well below those of $[SnCB_{10}H_{11}]^-$, and are thus capable of binding one or two σ-donor ligands, but are poor σ-donors themselves. In contrast, the frontier orbital energies of $[SnB_{11}H_{11}]^{2-}$ are quite high in energy, resulting in excellent σ-donor but poor π-acceptor behavior, accounting for the strong *trans*-influence of this ligand, and its ability to stabilize metals in unusually high oxidation states. The higher negative charge in the non-carbon containing systems, as well as the fact that boron is more electropositive than carbon, contribute to the increased energies of both HOMO and LUMO in the stannaboranes compared with the stannacarboranes, explaining their relative donor and acceptor properties.

Acknowledgement

References

1. D. Joosten, I. Weissinger, M. Kirchmann, C. Maichle-Mössmer, F.M. Schappacher, R. Pöttgen, and L. Wesemann. Organometallics **26**, 5696 (2007).
2. A.R. Rossi and R. Hoffmann. Inorg. Chem. **14**, 365 (1975).
3. M. Kretschmer, P.S. Pregosin, and J. Rüegger. J. Organomet. Chem. **241**, 87 (1983).
4. (a) J.A. Long, T.B. Marder, P.E. Behnken, and M.F. Hawthorne. J. Am. Chem. Soc. **106**, 2979 (1984); (b) see also: R.R. Schrock and J.A. Osborn. J. Am. Chem. Soc. **93**, 2397 (1971).
5. R.W. Chapman, J.G. Kester, K. Folting, W.E. Streib, and L.J. Todd. Inorg. Chem. **31**, 979 (1992).
6. T. Gädt and L. Wesemann. Z. Anorg. Allg. Chem. **633**, 693 (2007).
7. T. Marx, L. Wesemann, S. Dehnen, and I. Pantenburg. Chem. Eur. J. **7**, 3025 (2001).
8. (a) T. Gädt and L. Wesemann. Organometallics **26**, 2474 (2007). (b) S. Hagen, H. Schubert, C. Maichle-Mössmer, I. Pantenburg, F. Weigend, and L. Wesemann. Inorg. Chem. **46**, 6775 (2007). (c) T. Gädt and L. Wesemann. Dalton Trans. 328 (2006). (d) T. Gädt, L Eichele, and L. Wesemann. Dalton Trans. 2706 (2006). (e) S. Hagen, L. Wesemann, and I. Pantenburg. Chem. Commun. 1013 (2003). (f) T. Marx, B. Mosel, I. Pantenburg, S. Hagen, H. Shulze, and L. Wesemann. Chem. Eur. J. **9**, 4472 (2003). (g) S. Hagen, I. Pantenburg, F. Weigend, C. Wickleder, and L. Wesemann. Angew. Chem. Int. Ed. **42**, 1501

(2003). (h) L. Wesemann, S. Hagen, T. Marx, I. Pantenburg, M. Nobis, and D. Drießen-Hölscher. Eur. J. Inorg. Chem. 2261 (2002).

9. (a) M. Kirchmann, K. Eichele, F.M. Schappacher, R. Pöttgen, and L. Wesemann. Angew. Chem. Int. Ed. **47**, 963 (2008). (b) For a Highlight, see: S. Aldridge. Angew. Chem. Int. Ed. **47**, xxx (2008), DOI: 10.1002/anie.200705764.

10. (a) R.L. Voorhees and R.W. Rudolph. J. Am. Chem. Soc. **91**, 2173 (1969); (b) R.W. Rudolph and V. Chowdhry. Inorg. Chem. **13**, 248 (1974).

11. R.W. Rudolph, R.L. Voorhees, and R.E. Cochoy. J. Am. Chem. Soc. **92**, 3351 (1970).

12. T.B. Marder and M.F. Hawthorne. unpublished results, 1976.

13. A.H. Cowley, P. Galow, N.S. Hosmane, P. Jutzi, and N.C. Norman. J. Chem. Soc., Chem. Commun. 1564 (1984).

14. P. Jutzi, P. Galow, S. Abu-Orabi, A.M. Arif, A.H. Cowley, and N.C. Norman. Organometallics **6**, 1024 (1987).

15. N.S. Hosmane, P. de Meester, N.N. Maldar, S.B. Potts, S.S.C. Chu, and R.H. Herber. Organometallics **5**, 772 (1986).

16. R.D. Barreto, T.P. Fehlner, and N.S. Hosmane. Inorg. Chem. **27**, 453 (1988).

17. (a) U. Siriwardane, N.S. Hosmane, and S.S.C. Chu. Acta Crystallogr. **C43**, 1067 (1987). (b) J.A. Maguire, G.P. Ford, and N.S. Hosmane. Inorg. Chem. **27**, 3354 (1988). (c) N.S. Hosmane, M.S. Islam, U. Siriwardane, J.A. Maguire, and C.F. Campana. Organometallics **6**, 2447 (1987).

18. N.S. Hosmane, R.D. Barreto, M.A. Tolle, J.J. Alexander, W. Quintana, U. Siriwardane, S.G. Shore, and R.E. Williams, Inorg. Chem. 29, 2698 (1990).

19. N.S. Hosmane, N.S. Sirmokadam, and R.H. Herber. Organometallics **3**, 1665 (1984).

20. K.-S. Wong and R.N. Grimes. Inorg. Chem. **16**, 2053 (1977).

21. N.S. Hosmane, L. Jia, H. Zhang, and J.A. Maguire, Organometallics **13**, 1411 (1994)

22. N.M.M. Wilson, D. Ellis, A.S.F. Boyd, B.T. Giles, S.A. Macgregor, G.M. Rosair, and A.J. Welch. Chem. Commun. 464 (2002).

23. K. Nestor, B. Štíbr, T. Jelínek, and J.D. Kennedy. J. Chem. Soc., Dalton Trans. 1661 (1993).

24. K.-H. Wong, H.-S. Chan, and Z. Xie. Organometallics **22**, 1775 (2003).

25. M.J. Frisch, G.W. Trucks, H.B. Schlegel, G.E. Scuseria, M.A. Robb, J.R. Cheeseman, J.A. Montgomery, Jr., T. Vreven, K.N. Kudin, J.C. Burant, J.M. Millam, S.S. Iyengar, J. Tomasi, V. Barone, B. Mennucci, M. Cossi, G. Scalmani, N. Rega, G.A. Petersson, H. Nakatsuji, M. Hada, M. Ehara, K. Toyota, R. Fukuda, J. Hasegawa, M. Ishida, T. Nakajima, Y. Honda, O. Kitao, H. Nakai, M. Klene, X. Li, J.E. Knox, H.P. Hratchian, J.B. Cross, C. Adamo, J. Jaramillo, R. Gomperts, R.E. Stratmann, O. Yazyev, A.J. Austin, R. Cammi, C. Pomelli, J.W. Ochterski, P.Y. Ayala, K. Morokuma, G.A. Voth, P. Salvador, J.J. Dannenberg, V.G. Zakrzewski, S. Dapprich, A.D. Daniels, M.C. Strain, O. Farkas, D.K. Malick, A.D. Rabuck, K. Raghavachari, J.B. Foresman, J.V. Ortiz, Q. Cui, A.G. Baboul, S. Clifford, J. Cioslowski, B.B. Stefanov, G. Liu, A. Liashenko, P. Piskorz, I. Komaromi, R.L. Martin, D.J. Fox, T. Keith, M.A. Al-Laham, C.Y. Peng, A. Nanayakkara, M. Challacombe, P.N.W. Gill, B. Johnson, W. Chen, M.W. Wong, C. Gonzalez, and J.A. Pople. Gaussian 03, Revision C.02, Gaussian, Inc., Wallingford CT, 2004.

26. (a) A.D. Becke. J. Chem. Phys. **98**, 5648 (1993); (b) C. Lee, W. Yang, and R.G. Parr. Phys. Rev. B **37**, 785 (1988).

27. (a) G.A. Petersson and M.A. Al-Laham. J. Chem. Phys. **94**, 6081 (1991); (b) G.A. Petersson, A. Bennett, T.G. Tensfeldt, M.A. Al-Laham, W.A. Shirley, and J. Mantzaris. J. Chem. Phys. **89**, 2193 (1988).

28. (a) T.H. Dunning Jr., P.J. Hay. in *Modern Theoretical Chemistry*, H. F. Schaefer III, Ed., Vol. 3 (Plenum, New York, 1976); (b) P.J. Hay and W.R. Wadt. J. Chem. Phys. **82**, 270 (1985); (c) W.R. Wadt and P.J. Hay. J. Chem. Phys. **82**, 284 (1985); (d) P.J. Hay and W.R. Wadt. J. Chem. Phys. **82**, 299 (1985).

29. A.R. Allouche. Gabedit 2.1.0, CNRS et Université Claude Bernard Lyon1, 2007. Available at http://gabedit.sourceforge.net.

30. N.M. O'Boyle and J.G. Vos. GaussSum 1.0, Dublin City University, 2005. Available at http://gausssum.sourceforge.net.

31. R. McIntosh, D. Ellis, J. Gil-Lostes, K.J. Dalby, G.M. Rosair, and A.J. Welch. Dalton Trans. 1842 (2005).

32. (a) M. Bühl and P.v.R. Schleyer. J. Am. Chem. Soc. **114**, 477 (1992). (b) M. A. Fox, A.E. Goeta, A.K. Hughes, and A.L. Johnson. J. Chem. Soc., Dalton Trans. 2132 (2002).

33. (a) E.S. Alekseyeva, A.S. Batsanov, L.A. Boyd, M. A. Fox, T.G. Hibbert, J.A.K. Howard, J.A.H. MacBride, A. Mackinnon, and K. Wade. Dalton Trans. 475 (2003). (b) A.R. Turner, H.E. Robertson, K.B. Borisenko, D.W.H. Rankin, and M. A. Fox. Dalton Trans. 1310 (2005).

34. (a) J. Campbell, H.P.A. Mercier, H. Franke, D.P. Santry, D.A. Dixon, and G.J. Schrobilgen. Inorg. Chem. **41**, 86 (2002). (b) Y. Mizuhata, N. Takeda, T. Sasamori, and N. Tokitoh. Chem. Commun. 5876 (2005).

Table 1. Comparison of Sn-B and Sn-C bond distances between optimised gas-phase and reported experimental solid-state geometries, where available

		exp	calc
$[SnB_{11}H_{11}]^{2-}$	Sn-B (averaged) [a]	2.385(4)	2.395
$[SnCB_{10}H_{11}]^{-}$	Sn-C(1) [b]	2.466(5)	2.445
	Sn-B(3,6) (averaged)	2.415(6)	2.402
	Sn-B(7,11) (averaged)	2.380(5)	2.372
$3,1,2-SnC_2B_9H_{11}$	Sn-C(1,2)		2.515
	Sn-B(4,7)		2.399
	Sn-B(8)		2.345
$1,2-Me_2-3,1,2-SnC_2B_9H_9$	Sn-C(1,2)		2.546
	Sn-B(4,7)		2.383
	Sn-B(8)		2.323
$1,6-Me_2-4,1,6-SnC_2B_{10}H_{10}$	Sn-C(1) [c]	2.411(3)	2.396
	Sn-B(2)	2.639(4)	2.616
	Sn-B(3)	2.592(4)	2.585
	Sn-B(7)	2.453(4)	2.427
	Sn-C(6)	2.672(4)	2.678
	Sn-B(10)	2.425(4)	2.403
$2-Me_3Si-1,2,3-SnC_2B_4H_5$	Sn-C(2) [d]	2.518(5)	2.488
	Sn-C(3)	2.475(6)	2.456
	Sn-B(4)	2.432(7)	2.438
	Sn-B(5)	2.397(8)	2.404
	Sn-B(6)	2.431(7)	2.434

[a] Ref. 6.
[b] Ref. 1.
[c] Ref. 22. Poor quality X-ray structural data for $4,1,6-SnC_2B_{10}H_{10}$ have also been reported.
[d] Refs. 13 and 15.

Table 2. Molecular orbital coefficients and energies for [SnB$_{11}$H$_{11}$]$^{2-}$

MO		eV	Sn	BH(upper)	BH(lower)	BH(unique)
41	**L+4**	**9.50**	**0**	**57**	**42**	**1**
40	**L+3**	**9.50**	**0**	**57**	**42**	**1**
39	L+2	8.53	75	16	9	0
38	**L+1**	**7.23**	**81**	**10**	**6**	**4**
37	**LUMO**	**7.23**	**81**	**10**	**6**	**4**
36	HOMO	1.44	23	57	16	4
35	H-1	1.43	32	48	15	5
34	H-2	1.43	53	27	14	6
33	**H-3**	**0.71**	**0**	**56**	**44**	**0**
32	**H-4**	**0.71**	**0**	**56**	**44**	**0**

Note that degenerate levels are shown in bold.

Table 3. Molecular orbital coefficients and energies for [SnCB$_{10}$H$_{11}$]$^{-}$

MO		eV	Sn	CH	BH(upper)	BH(lower)	BH(unique)
41	L+4	5.23	1	2	49	47	1
40	L+3	5.08	6	11	39	43	1
39	L+2	4.35	69	5	14	11	1
38	L+1	2.93	77	2	8	8	5
37	LUMO	2.45	84	5	2	7	3
36	HOMO	-2.87	46	2	30	16	7
35	H-1	-2.87	20	1	58	17	4
34	H-2	-3.54	12	3	48	34	3
33	H-3	-3.80	0	0	28	63	8
32	H-4	-3.90	5	2	31	48	15

Table 4. Molecular orbital coefficients and energies for 3,1,2-SnC$_2$B$_9$H$_{11}$

MO		eV	Sn	CH	BH(upper)	BH(lower)	BH(unique)
41	L+4	0.78	4	5	39	51	1
40	L+3	0.41	5	23	23	45	3
39	L+2	0.00	66	9	11	12	2
38	L+1	-1.99	76	8	2	11	3
37	LUMO	-2.30	87	2	2	7	2
36	HOMO	-7.33	39	3	32	18	9
35	H-1	-7.65	14	11	48	24	3
34	H-2	-8.21	1	3	26	64	6
33	H-3	-8.32	1	2	40	44	13
32	H-4	-8.41	2	1	32	56	10

Table 5. Molecular orbital coefficients and energies for [SnCl₃]⁻

MO		eV	Sn	Cl$_3$
33	**L+4**	**9.67**	**97**	**3**
32	**L+3**	**9.67**	**97**	**3**
31	L+2	3.43	87	13
30	**L+1**	**3.25**	**95**	**5**
29	**LUMO**	**3.25**	**95**	**5**
28	HOMO	-2.45	45	55
27	H-1	-3.56	0	100
26	**H-2**	**-3.67**	**2**	**98**
25	**H-3**	**-3.67**	**2**	**98**
24	H-4	-3.97	0	100

Note that degenerate levels are shown in bold.

Table 6. Molecular orbital coefficients and energies for PF₃

MO		eV	P	F$_3$
26	L+4	8.1	94	6
25	L+3	6.21	106	-5
24	L+2	2.94	92	8
23	**L+1**	**-0.11**	**92**	**8**
22	**LUMO**	**-0.11**	**92**	**8**
21	HOMO	-8.78	64	36
20	H-1	-11.48	0	100
19	**H-2**	**-11.85**	**4**	**96**
18	**H-3**	**-11.85**	**4**	**96**
17	H-4	-12.81	4	96

Note that degenerate levels are shown in bold.

Table 7. Molecular orbital coefficients and energies for CO

MO		eV	C	O
12	**L+4**	**13.93**	**100**	**0**
11	**L+3**	**13.93**	**100**	**0**
10	L+2	7.14	144	-43
9	**L+1**	**-0.59**	**76**	**24**
8	**LUMO**	**-0.59**	**76**	**24**
7	HOMO	-10.11	90	10
6	**H-1**	**-12.72**	**27**	**73**
5	**H-2**	**-12.72**	**27**	**73**
4	H-3	-15.51	21	79
3	H-4	-31.51	26	74

Note that degenerate levels are shown in bold.

Table 8. Calculated LUMO and HOMO energies for known dicarbastannaboranes

	LUMO	HOMO
1,2,3-SnC$_2$B$_4$H$_6$ [a]	-1.64	-6.73
1,2,4-SnC$_2$B$_4$H$_6$ [b]	-1.69	-6.93
1,2,3-SnC$_2$B$_8$H$_{10}$ [c]	-2.25	-7.32
3,1,2-SnC$_2$B$_9$H$_{11}$ [d]	-2.30	-7.33
4,1,6-SnC$_2$B$_{10}$H$_{12}$ [e]	-2.55	-7.37
1,2-μ-(CH$_2$CH=CHCH$_2$)-4,1,2-SnC$_2$B$_{10}$H$_{10}$ [f]	-2.72	-7.22

[a] Ref. 20.
[b] For 2,4-(Me$_3$Si)$_2$-1,2,4-SnC$_2$B$_4$H$_6$ see ref. 21.
[c] Ref. 23.
[d] Refs. 10 and 11.
[e] Ref. 22.
[f] For 1,2-[μ-C$_6$H$_4$(CH$_2$)$_2$]-4,1,2-SnC$_2$B$_{10}$H$_{10}$ see ref. 24.

Table 9. Comparison of calculated and observed (where available) ^{11}B, ^{13}C and ^{1}H NMR chemical shifts

	[11]B, ^{13}C calc	[11]B, ^{13}C exp	[1]H calc	[1]H exp
$[SnB_{11}H_{11}]^{2-}$	-7.6 (B12)	-5.5 (B12) [a]	2.38 (B12H)	
	-12.3 (B2-6)	-10.9 (B2-6)	1.97 (B7-11H)	
	-14.7 (B7-11)	-12.2 (B7-11)	1.30 (B2-6H)	
$[2,1-SnCB_{10}H_{11}]^-$	-6.6 (B12)	-6.0 (1B) [b]	2.58 (B9H)	3.53 (1H) [b]
	-7.6 (B9)	-7.1 (1B)	2.45 (B12H)	2.20 (1H)
	-9.6 (B7,11)	-8.3 (2B)	2.39 (B8,10H)	2.11 (2H, B8,10H)
	-11.5 (B8,10)	-10.5 (2B, B8,10)	2.36 (B4,5H)	2.04 (2H)
	-16.2 (B4,5)	-14.6 (2B)	1.74 (B3,6H)	1.38 (2H, B3,6H)
	-16.8 (B3,6)	-15.3 (2B, B3,6)	1.52 (B7,11H)	0.99 (2H)
	51.5	*51.8*	1.66 (CH)	1.76 (CH)
$3,1,2-SnC_2B_9H_{11}$	-2.0 (B9,12)		3.06 (B9,12H)	
	-5.6 (B8)	-6.8 [c]	2.98 (B6H)	
	-8.0 (B10)		2.90 (B10H)	
	-12.1 (B5,11)		2.78 (B5,11H)	
	-14.0 (B6)	-13.8	2.12 (B8H)	
	-15.8 (B4,7)		1.92 (B4,7H)	
	47.7		2.74 (CH)	
1,2-Me₂-3,1,2-SnC₂B₉H₉	-2.6 (B9,12)		2.99 (B9,12H)	
	-3.4 (B6)	-3.9 (4B) [d]	2.98 (B5,11H)	
	-3.8 (B8)		2.85 (B6H)	
	-6.9 (B5,11)	-5.9 (2B)	2.72 (B10H)	
	-10.1 (B4,7)	-8.5 (2B)	2.42 (B4,7H)	
	-10.7 (B10)	-12.4 (1B)	1.91 (B8H)	
	72.2 (cage C)	*69.4 (cage C)*	2.02 (CH₃)	1.69 (CH₃) [d]
	25.4 (CH₃)	*26.5 (CH₃)*		
$4,1,6-SnC_2B_{10}H_{12}$	17.8 (B3) [e]		4.69 (B8H) [e]	
	15.8 (B8)	11.3 (1B) [f]	4.63 (B2H)	
	9.5 (B11)	10.7 (2B)	3.96 (B13H)	
	8.5 (B2)	9.1 (2B)	4.29 (B3H)	
	7.5 (B9)		4.10 (B9H)	
	6.9 (B13)		3.81 (B12H)	
	6.0 (B7)	7.3 (3B)	3.60 (B7H)	
	1.9 (B12)		3.05 (B11H)	
	-3.4 (B10)		1.41 (B10H)	
	-13.4 (B5)	-6.3 (2B)	0.91 (B5H)	
			7.08 (C1H)	5.51 (CH) [f]
	118.3 (C1)	*92.3*	3.94 (C6H)	
	65.2 (C6)			
$4,1,6-SnC_2B_{10}H_{12}$	11.4 (B8,13) [g]	11.3 (1B) [f]	4.63 (B2H) [g]	
	9.5 (B11)	10.7 (2B)	4.33 (B8,13H)	
	8.5 (B2)	9.1 (2B)	4.10 (B9H)	
	7.5 (B9)		3.60 (B7H)	
	7.2 (B3,10)	7.3 (3B)	3.05 (B11H)	
	6.0 (B7)		2.85 (B3,10H)	
	-5.8 (B5,12)	-6.3 (2B)	2.36 (B5,12H)	
	90.1	*92.3*	5.51 (C1,6H)	5.51 (CH) [f]
$1,2,3-SnC_2B_8H_{10}$	-0.6 (B8,9)	0.5 (B8,9) [h]	3.42 (B10,11H)	3.83 (B8,9H) [h]
	-1.8 (B4,5,6,7)	0.2 (B4,5,6,7)	3.15 (B8,9H)	2.48 (B4,5,6,7H)
	-7.1 (B10,11)	-6.1 (B10,11)	3.15 (B4,5,6,7H)	1.96 (B10,11H)
	105.8		6.22 (CH)	6.28 (CH)

[a] Ref. 7.
[b] Ref. 1.

[c] Ref. 11.

[d] Ref. 14.

[e] Computed values are based on the ground-state optimized 'gas-phase' and experimental 'solid-state' asymmetric geometry.

[f] Ref. 22.

[g] Computed values are based on fluxionality between two ground-state asymmetric geometries in solution. Shifts for the pairs C1/6, B8/13, B5/12, B3/10 and their exo-hydrogens are averaged.

[h] Ref. 23.

Scheme 1. Schematic representations of the key compounds discussed in the paper. Solid circles represent C-H vertices whereas open circles represent B-H vertices.
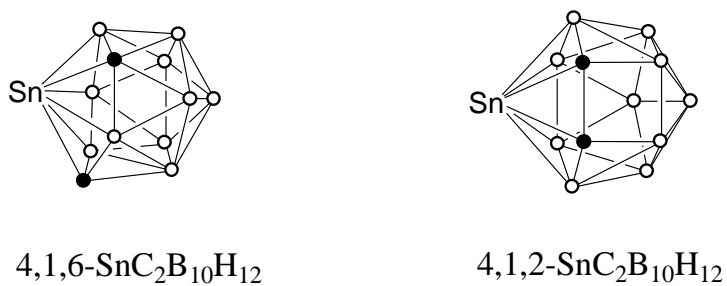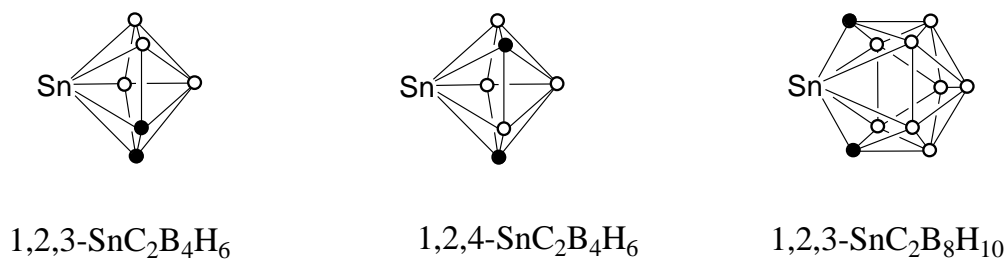

1

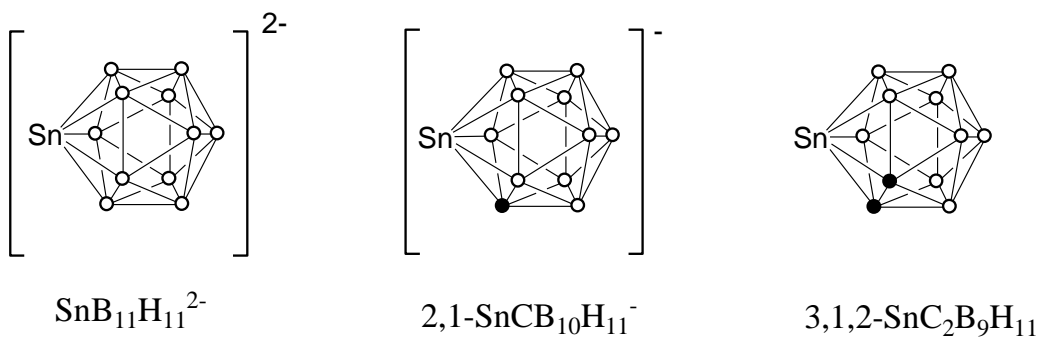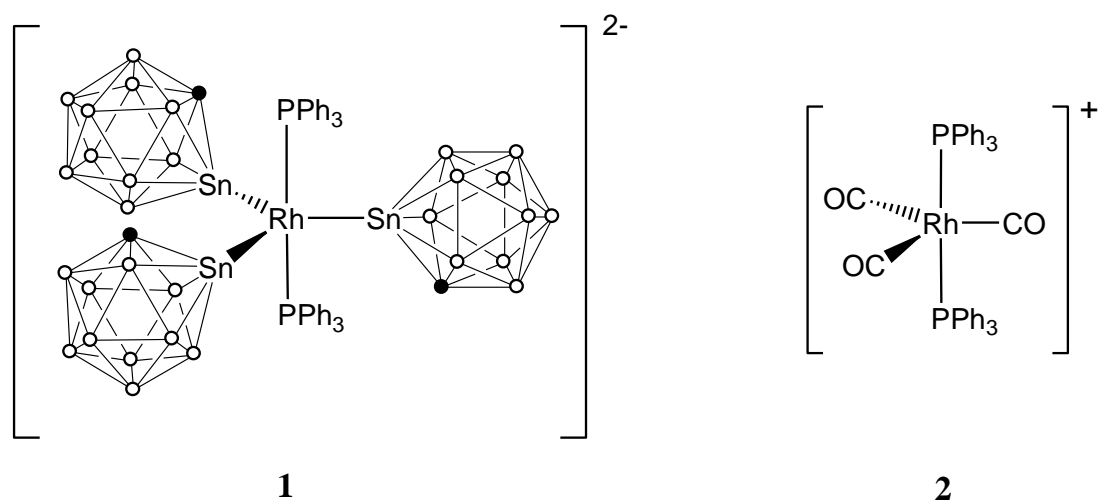**2**

$SnB_{11}H_{11}^{2-}$

$2,1\text{-}SnCB_{10}H_{11}^{-}$

$3,1,2\text{-}SnC_2B_9H_{11}$

$1,2,3\text{-}SnC_2B_4H_6$

$1,2,4\text{-}SnC_2B_4H_6$

$1,2,3\text{-}SnC_2B_8H_{10}$

$4,1,6\text{-}SnC_2B_{10}H_{12}$

$4,1,2\text{-}SnC_2B_{10}H_{12}$

Fig. 1. Frontier orbitals for $[SnB_{11}H_{11}]^{2-}$, $[SnCB_{10}H_{11}]^-$, and 3,1,2-$SnC_2B_9H_{11}$. Note that for $[SnB_{11}H_{11}]^{2-}$, LUMO and LUMO+1 constitute a degenerate pair, in contrast to $[SnCB_{10}H_{11}]^-$ and 3,1,2-$SnC_2B_9H_{11}$, for which there are no degeneracies.

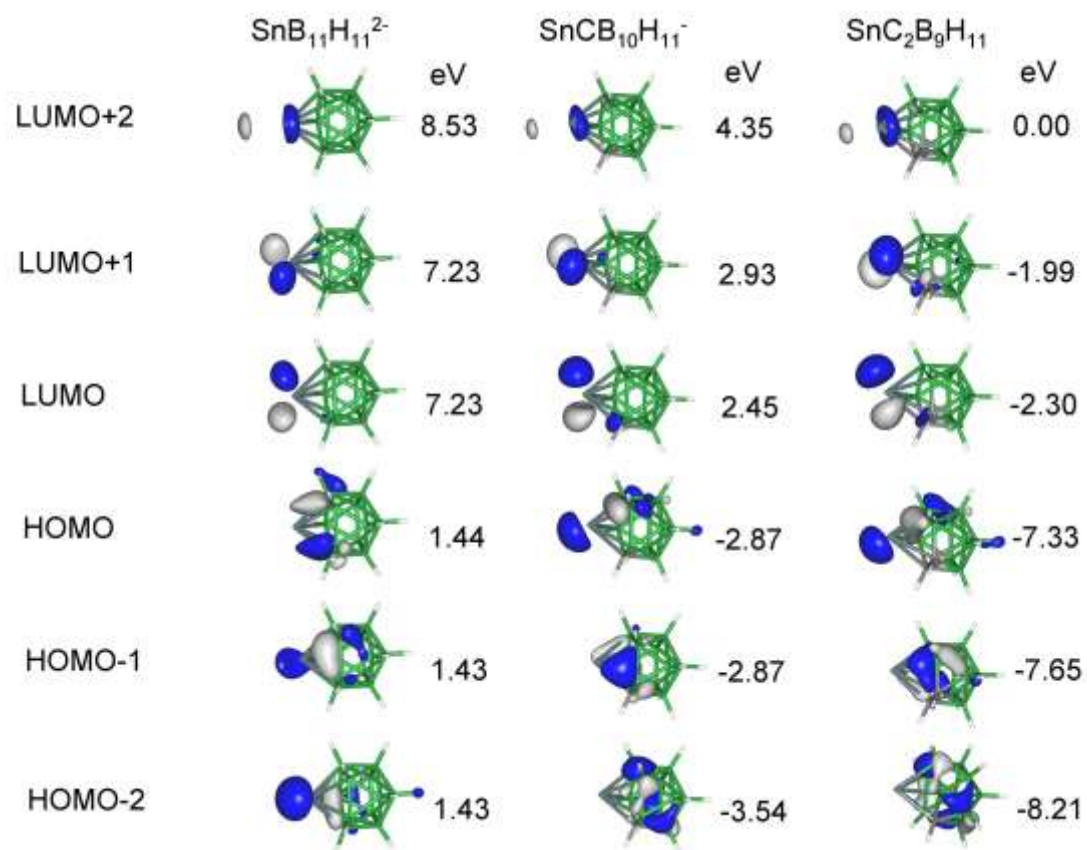|	$SnB_{11}H_{11}^{2-}$		$SnCB_{10}H_{11}^-$		$SnC_2B_9H_{11}$	
		eV		eV		eV
LUMO+2		8.53		4.35		0.00
LUMO+1		7.23		2.93		-1.99
LUMO		7.23		2.45		-2.30
HOMO		1.44		-2.87		-7.33
HOMO-1		1.43		-2.87		-7.65
HOMO-2		1.43		-3.54		-8.21

Fig. 2. Frontier orbitals for [SnCl$_3$]$^-$, PF$_3$, and CO. Note that orbitals labelled HOMO-1 and HOMO-2 are a degenerate pair as are LUMO and LUMO+1.

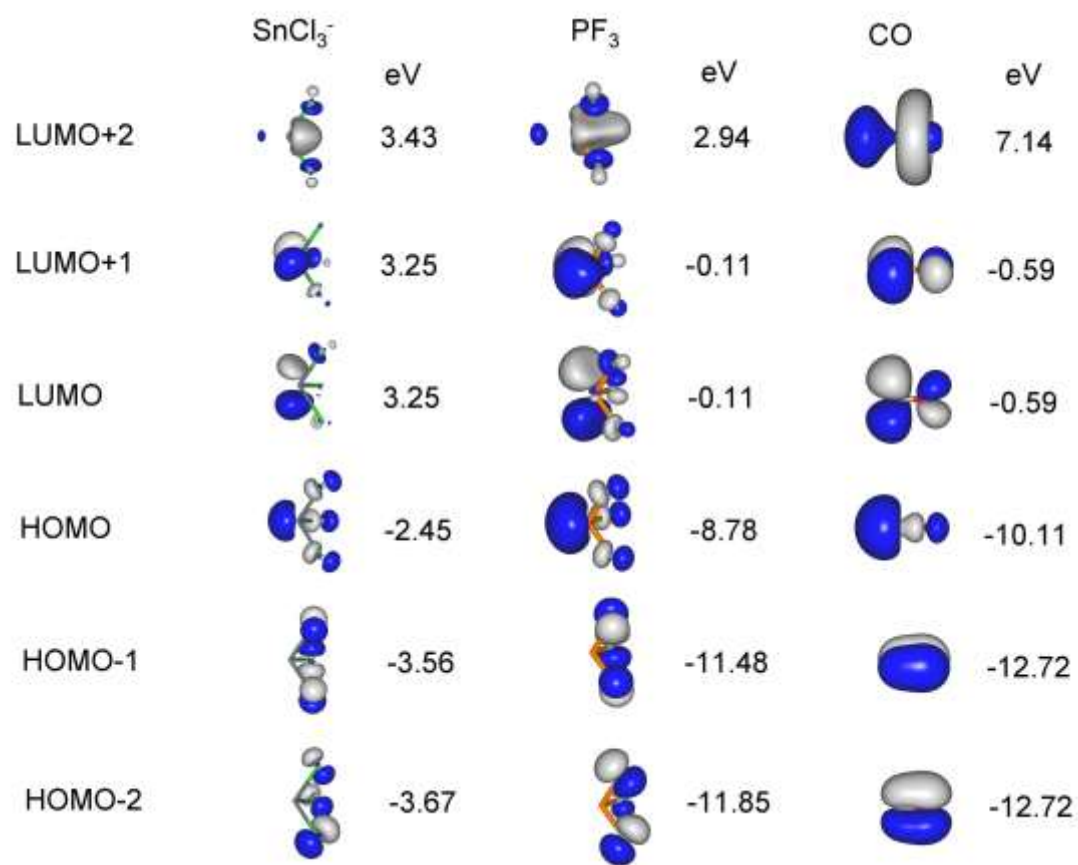|	SnCl$_3^-$		PF$_3$		CO	
		eV		eV		eV
LUMO+2		3.43		2.94		7.14
LUMO+1		3.25		-0.11		-0.59
LUMO		3.25		-0.11		-0.59
HOMO		-2.45		-8.78		-10.11
HOMO-1		-3.56		-11.48		-12.72
HOMO-2		-3.67		-11.85		-12.72

Table of Contents artwork:

	$[SnCB_{10}H_{11}]^-$		$[SnCl_3]^-$	
LUMO		2.45 eV		3.25 eV
HOMO		-2.87 eV		-2.45 eV